



Published in final edited form as:

Ann Rheum Dis. 2015 June ; 74(6): 1284–1292. doi:10.1136/annrheumdis-2013-204782.

IL-17A GENE TRANSFER INDUCES BONE LOSS AND EPIDERMAL HYPERPLASIA ASSOCIATED WITH PSORIATIC ARTHRITIS

IANNIS E. ADAMOPOULOS^{1,2,3,*}, ERIKA SUZUKI², CHENG-CHI CHAO¹, DAN GORMAN¹, SARVESH ADDA¹, EMANUAL MAVERAKIS⁴, KONSTANTINOS ZARBALIS^{3,5}, RICHARD GEISLER⁶, AGELIO ASIO¹, WENDY M BLUMENSCHIN¹, TERRILL McCLANAHAN¹, RENE DE WAAL MALEFYT¹, M. ERIC GERSHWIN², and EDWARD P. BOWMAN^{1,*}

¹Discovery Research, Merck Research Laboratories, Palo Alto

²Division of Rheumatology, Allergy and Clinical Immunology, University of California, Davis

³Institute for Pediatric Regenerative Medicine, Shriners Hospitals for Children Northern California

⁴Department of Dermatology, University of California, Davis, USA

⁵Department of Pathology and Laboratory Medicine, University of California, Davis

⁶Anatomic Pathology & Clinical Laboratory Departments, Stanford University, Palo Alto, CA, USA

Abstract

Background—Psoriatic arthritis (PsA) is a chronic inflammatory disease characterized by clinical features that include bone loss and epidermal hyperplasia. Aberrant cytokine expression has been linked to joint and skin pathology; however, it is unclear which cytokines are critical for disease initiation. IL-17A participates in many pathologic immune responses; however, its role in PsA has not been fully elucidated.

Objective—To determine the role of IL-17A in epidermal hyperplasia and bone destruction associated with psoriatic arthritis.

Design—An *in vivo* gene transfer approach was used to investigate the role of IL-17A in animal models of inflammatory (Collagen-induced arthritis) and non-inflammatory (RANKL-gene transfer) bone loss.

Results—IL-17A gene transfer induced the expansion of IL-17RA⁺CD11b⁺Gr1^{low} osteoclast precursors and a concomitant elevation of biomarkers indicative of bone resorption. This occurred at a time preceding noticeable joint inflammation suggesting that IL-17A is critical for the

* Correspondence and reprint requests to Iannis E Adamopoulos, Shriners Hospital for Children Northern California, Institute for Pediatric Regenerative Medicine, 2425 Stockton Blvd, Room 653A, Sacramento, CA 95817. iannis@ucdavis.edu Tel: 916-453-2237, Fax: 916-453-2000 and Edward P. Bowman, Department of Therapeutic Area Biology and Pharmacology, Merck Research Laboratories, 901 California Avenue, Palo Alto, CA 94304, USA. Eddie.Bowman@merck.com.

There are no other conflicts.

Competing interests

The study was partly funded by Merck and the authors IEA, CCC, DG, SA, RG, AG, WB, TM, RDWM and EPB were Merck employees at the time of the study.

induction of pathological bone resorption through direct activation of osteoclast precursors. Moreover, IL-17A induced a second myeloid population CD11b⁺Gr1^{high} neutrophil-like cells which was associated with cutaneous pathology including epidermal hyperplasia, parakeratosis, and Munro's microabscesses formation.

Conclusion—Collectively, these data support that IL-17A can play a key role in the pathogenesis of inflammation-associated arthritis and/or skin disease, as observed in PsA.

Keywords

Interleukin-17A; psoriatic arthritis; osteoclasts

INTRODUCTION

Psoriatic arthritis (PsA) is an inflammatory rheumatic disorder of unknown etiology occurring concurrently or before the onset of psoriasis. In PsA patients, psoriatic features of epidermal hyperplasia accompanied by parakeratosis (retention of keratinocyte nuclei in the stratum corneum) and neutrophilic exudates in the epidermis (Munro's microabscesses) are sometimes followed many years later by synovial inflammation, bone destruction, and juxta-articular new bone formation [1]. Bone destruction is the result of excess differentiation and/or activation of osteoclasts, a cell uniquely specialized to carry out bone resorption [2]. Osteoclast precursors circulate in peripheral blood and differentiate into multinucleated osteoclasts in the presence of macrophage-colony stimulating factor (M-CSF) and receptor activator for nuclear factor κ -B ligand (RANKL) [3, 4].

Interleukin 17A (IL-17A) together with other T helper 17 cell (T_h17)-related cytokines have been detected in the synovium and synovial fluid of rheumatoid patients, as well as in human psoriatic skin lesions [5–7]. IL-23, which plays a major role in T_h17-cell development and IL-17A production, stimulates epidermal hyperplasia, enthesitis, synovial inflammation and bone destruction in rheumatic disease models [8–10]. Although T_h17 cells have been implicated in the pathogenesis of psoriasis and PsA, the contribution of IL-17A versus IL-23 or other T_h17-related cytokines such as IL-22 remains puzzling [11–15]. Similarly, both IL-23 and IL-17A are also associated with changes in the RANKL-RANK axis and increased osteoclast formation that can lead to bone pathology [16–18]. Although IL-17A was not critical in experimental psoriasis-like skin inflammation, other reports showed that blockade of IL-17A or IL-17RA led to rapid clinical response in subjects with moderate-to-severe psoriasis [19, 20]. More recent evidence using IL-17A-committed γ 4⁺ γ δ T-cells highlighted a role of IL-17A in the development of psoriasis-like skin changes [21]. Taken together, a plethora of evidence suggests a role of IL-17A in PsA pathology via indirect mechanisms involving γ δ T-cells, epithelial, endothelial and fibroblastic cells.

In this paper, we demonstrate a direct role of IL-17A in expanding IL-17R⁺CD11b⁺Gr1^{low}RANK⁺CSF-1R⁺ osteoclast precursors, which are ultimately responsible for the bone destruction observed in inflammatory arthritis. Moreover, we show that IL-17A directly expands a CD11b⁺Gr1^{high} neutrophil-like cell subset associated with Munro's microabscesses and epidermal hyperplasia with associated parakeratosis typically observed in psoriasis. Both osteoclast-mediated bone resorption and epidermal hyperplasia

are hallmarks of PsA. Collectively our data support IL-17A as a possible target to combat PsA and reveal a novel link between IL-17 and cells of hematopoietic origin that are associated with joint and skin pathology observed in PsA.

METHODS

Mice and Reagents

Merck Research Labs and UC Davis Institutional Animal Care and Use Committee approved all animal protocols. C57BL/6J mice (The Jackson Laboratory, Sacramento, CA,) were sacrificed by carbon dioxide exposure and blood collected by cardiac puncture. All cell incubations were performed in culture medium consisting of alpha minimal essential medium (α MEM) (Invitrogen, USA), 2 mM glutamine, 10% heat-inactivated fetal bovine serum (Invitrogen), 100 IU/ml penicillin and 100 μ g/ml streptomycin. Mouse M-CSF and RANKL, RANKL and IL-17A ELISA were purchased from R&D Systems (USA). Serum CTX-I and TRAP5b were measured using a RatLaps-EIA kit from Nordic Bioscience Diagnostics A/S and ELISA from Sigma (St Louis, USA), respectively. APC-conjugated anti-mouse CD115 (AFS98), PE-Cy5-conjugated anti-mouse Gr-1 (RB6-8C5), Pacific blue-conjugated anti-mouse CD11b (M1/70), biotin-conjugated anti-mouse RANK (R12-31), Streptavidin 605 violet, Biotin and PE rat IgG2a isotypes (RTK2758), and PE-conjugated anti-mouse RANK (R12-31) were all purchased from Biolegend.

Production and purification of minicircle DNA

Mouse IL-17A and RANKL minicircle-DNA constructs were produced according to methods described previously [22] and adjusted to 1L culture volume. Single isolated colony from a fresh plate was grown for 8 hr in 2 ml Luria-Bertani broth with ampicillin. Inoculated 800 μ l of this culture onto 1L of Terrific broth and grown for additional 17 hrs. Overnight cultures were centrifuged at 20 °C 4000 rpm for 20 minutes. The pellet was resuspended 4:1 (v/v) in fresh Luria-Bertani broth containing 1% L-arabinose. The bacteria were incubated at 32 °C with constant shaking at 250 rpm for 2 hours. After adding one-half volume of fresh low salt Luria-Bertani broth (pH 8.0) containing 1% L-arabinose, the incubation temperature was increased to 37°C and the incubation continued for an additional 2 hours. Episomal DNA circles were prepared from bacteria using the Endofree Qiagen Megaprep plasmid purification kits (Chatsworth, CA) and sequences were verified by sequencing on an ABI3130x1 Genetic analyzer. 8 μ g MC DNA were used for IL-17A and GFP and 0.5 μ g for RANKL in all further experiments. Whole body and liver explant images 24 hrs post-gene transfer were obtained using a solid-state liquid crystal tunable filter-based imaging technology, Maestro 2 (Cri).

Flow cytometry of isolated bone marrow macrophages and splenocytes

Bone marrow and spleen cells were isolated from C57BL/6J mice 3 days post gene transfer of either GFP or IL-17A MC. Spleens were treated with collagenase (Sigma) for 15 min at 37°C and then washed with FBS-containing media. Cells were dispersed into single-cell suspensions using a 70 micron nylon mesh (Fisher), washed and resuspended in 1–3 ml of ACK lysis buffer (Quality Biological, MD, USA) on ice for 3 min. Non-specific binding was blocked by pretreating cells with rat anti-mouse CD16/32 mAb (clone 2.4G2 BD

Biosciences, San Jose, CA, USA) for 10 minutes at room temperature. Cells were stained using predetermined optimized mAb concentration, and events (1,000,000) were collected on a FACS Aria II flow cytometer (BD Biosciences) and were analyzed using FlowJo software (Tree Star, Ashland, OR, USA).

Mouse osteoclast cultures

Cells unlabeled or labeled with anti-RANK were sorted using FACS Aria II cell sorter (BD Biosciences). Cells were washed and cultured on 5 mm glass coverslips in a 96-well plate at 37 °C with 5% CO₂ for 4 days in the presence of M-CSF (25 ng/ml) and/or RANKL (60 ng/ml). The cells cultured on plastic dishes were stained for TRAP using a commercial kit (387-A, Sigma) according to manufacturer's instructions. F-actin rings were visualized as previously described [9].

Collagen-induced arthritis (CIA)

Female C57BL/6J mice (The Jackson Laboratory, Sacramento, CA, USA) were injected with either GFP or IL-17A MC DNA 3 days before getting immunized with chicken type II collagen (CII) (Sigma-Aldrich, St. Louis, MO) emulsified intradermally with complete Freund's adjuvant (DIFCO, Detroit, MI). 50 µL of 1 mg/ml CII/CFA emulsion was injected on both sides of the tail base. Mice were challenged intradermally 21 days later with 1 mg/ml CII emulsified in incomplete Freund's adjuvant. Mice were observed daily before and after the first signs of swollen paws within the cohort scored and processed for micro-computed tomography imaging (µCT) as previously described [23].

Transmission Electron Microscopy (TEM)

Skin samples taken from dorsal skin were fixed overnight in buffered 2.5% glutaraldehyde and 2% formaldehyde, washed in buffer, dehydrated in an ethanol series and flat embedded in epoxy resin. One-micrometer sections for light microscopy, stained with methylene blue & azure II were reviewed with selected areas thin sectioned then stained with uranyl acetate and lead citrate. Transmission electron microscopic imaging was performed with an FEI, Inc. model CM10 equipped with a Gatan Orius camera system.

RNA extraction and real-time quantitative PCR

Total RNA was purified from different stages of osteoclast cultures using the RNeasy Mini Kit (QIAGEN). Gene expression was calculated using the $-Ct$ method (using the mean cycle threshold value for ubiquitin and the gene of interest for each sample). The equation $1.8e^{(Ct \text{ ubiquitin} - Ct \text{ gene of interest})} \times 10^4$ was used to obtain the normalized values.

Statistical analysis

Data were analyzed by Student's t-test and Mann-Whitney non-parametric tests as indicated in the figure legends of each assay. One-way or two-way ANOVA with Bonferroni after test were used where appropriate. $p < 0.05$ was considered to be statistically significant ($n = 3$, unless otherwise indicated).

RESULTS

IL-17A gene transfer *in vivo* induces two distinct myeloid populations

A recombinant minicircle (MC) construct encoding the IL-17A gene (see online supplementary Figure S1) was injected hydrodynamically into the tail vein to establish systemic expression of IL-17A *in vivo* due to transduction of hepatocytes [9, 22]. A green fluorescent protein (GFP) minicircle DNA construct was also injected hydrodynamically as a negative control and could be visualized 24 hours after injection using a 2D fluorescence imager Maestro 2 (Figure 1a, b). Stable systemic expression of IL-17A was established with 4 or 8 μ g of MC DNA. Quantification of serum IL-17A taken from periodic tail bleeds demonstrated that IL-17A was stably expressed for a period of at least 24 weeks (Figure 1c). Within 7 days of gene transfer, we observed the expansion of a CD11b⁺Gr1^{low} myeloid population in the bone marrow (Mean \pm SD; GFP MC: 19 \pm 3%, IL-17A MC: 40 \pm 4% $p < 0.01$) and spleen (GFP MC: 8 \pm 1%, IL-17A MC: 13 \pm 1% $p < 0.01$). Additionally, a second myeloid population consisting of CD11b⁺Gr1^{high} cells was also expanded in both the bone marrow (GFP MC: 25 \pm 3%, IL-17A MC: 38 \pm 4% $p < 0.01$) and spleen (GFP MC: 0.6 \pm 0.3%, IL-17A MC: 2.4 \pm 0.6% $p < 0.01$). Thus, IL-17A induces the expansion of both CD11b⁺Gr1^{low} and CD11b⁺Gr1^{high} populations (Figure 1d, e). These data were recorded within 7 days post-gene transfer, at a timepoint when other cytokines were not detectably elevated in the serum by a multiplex bead array assay from an extensive cytokine panel including MIP-3 α , IFN γ , GM-CSF, IL-4, IL-6, IL-10, IL-17E, IL-17F, IL-21, IL-23, IL-27, and TNF (tumor necrosis factor). IL-17A and IL-17E were the only two cytokines that were elevated compared to GFP controls for the first 7 days post-gene transfer. Subsequent serum analysis at week 7 post-gene transfer revealed a more generalized pro-inflammatory cytokine signature (Figure 1f).

IL-17A expands IL-17R⁺CD11b⁺Gr1^{low}RANK⁺CSF-1R⁺ osteoclast precursors and exacerbates RANKL-mediated osteoclastogenesis

To characterize the pathological potential of systemic IL-17A expression and the contribution of secondary cytokines downstream of IL-17A in synovial inflammation and bone destruction, we examined hematoxylin and eosin (H&E) stained decalcified limb samples from the IL-17A MC-injected mice at 7 weeks after gene transfer. There was no evidence of visual paw swelling, nor was histological joint inflammation observed (Figure 2a). Surprisingly, IL-17A MC injected mice showed signs of systemic bone erosion by micro-computed tomography (μ CT) in the absence of overt inflammation (Figure 2b) and the increased bone resorption correlated with a significant increase in serum TRAP5b with serum RANKL remaining unchanged (Figure 2c, d).

To further investigate this observation we isolated CD11b⁺ cells from bone marrow and spleen of GFP MC or IL-17A MC injected animals and characterised them by flow cytometry. Our data show that IL-17A gene transfer induced the key osteoclastogenic receptors RANK (Mean \pm SD) (1.5% \pm 0.1%) and CSF-1R (13% \pm 1.1%) in the bone marrow (Figure 2e) and in the spleen (1.0% \pm 0.2 and 2.0% \pm 0.2 respectively) (Figure 2f). Since both of these receptors are crucial in the differentiation of monocytes to

osteoclasts [24]; next we sought to identify if the changes in RANK expression in osteoclast precursors affected the rate of osteoclastogenesis *in vivo*.

Carboxy-terminal collagen crosslinks (CTX-I) in serum (a marker of bone resorption) showed a non-significant increased trend in the IL-17A MC over GFP MC which probed us to investigate the effect of IL-17A on bone destruction further (see online supplementary Figure S2a, b). A RANKL expressing mini-circle vector was injected hydrodynamically to establish systemic expression of RANKL *in vivo* in IL-17A or GFP overexpressing C57BL/6 mice (see online supplementary Figure S2c). These experiments showed that mice with double gene transfer of IL-17A and RANKL had significantly elevated TRAP5b which persisted 11 days ($p=0.0022$) and 38 days ($p=0.0166$) post-RANKL gene transfer (Figure 2g).

IL-17A induces osteoclast differentiation in a RANKL dependent manner *in vitro*

To validate our *in vivo* findings we performed osteoclast assays *in vitro* by culturing bone marrow macrophages in the presence of MCSF and RANKL. RANK⁺ sorted bone marrow macrophages from IL-17A MC injected mice showed a marked increase in multinucleated TRAP⁺ cells that were capable of F-actin ring formation compared to GFP MC controls (Figure 3a, b, c). This also correlated with a marked increase of *Il-17ra*, *Csf1r* and *Nfatc1* mRNA compared to GFP MC controls (Figure 3d). Finally, flow cytometric analysis revealed an increase of RANK expression on cells extracted from bone marrow after IL-17A MC injection relative to GFP MC controls (Figure 3e).

IL-17A exacerbates synovial inflammation and bone loss in inflammatory arthritis

Next we sought to investigate the effect of systemic IL-17A in inflammatory arthritis by performing IL-17A gene-transfer in a collagen-induced arthritis (CIA) mouse model. Gene transfer of IL-17A exacerbated arthritis disease severity based on paw swelling and initiated arthritis at much earlier timepoints as compared to GFP MC controls (Figure 4a, b). H&E-stained decalcified limb samples of IL-17A gene transfer mice revealed a hyperplastic and inflamed synovium, which contained a mixed inflammatory infiltrate consisting of mononuclear cells and numerous polymorphonuclear leukocytes. Neovascularization and proliferation of fibrocellular pannus was also pronounced. In some areas, the pannus had eroded into adjacent cartilage, and occasionally completely obliterated the normal joint architecture as confirmed by μ CT (Figure 4c, d). In addition to using visual paw swelling scores, histology scores confirmed exacerbated histological parameters of arthritis including pannus formation, reactive synovium, leukocyte infiltration, cartilage proliferation, and bone erosion and destruction (see online supplementary Figure S3). The prominent bone destruction correlated with a significant increase of *Rankl*, *Trap*, and *Mmp9* mRNA levels in keeping with an osteoclast signature (Figure 4e).

Systemic IL-17A induces cutaneous disease

We examined H&E-stained ear and dorsal skin samples from IL-17A MC-injected mice 7 weeks post-gene transfer to characterize the potential role of systemic IL-17A in skin inflammation. IL-17A gene transfer resulted in diffuse epidermal hyperplasia (acanthosis) with associated compact hyperkeratotic and parakeratosis of the stratum corneum (Figure

5a). The visual skin pathology occurred randomly within a cohort of IL-17A MC-injected mice between 5 days to 8 weeks post-transfer and occurred on the ears, face, behind the neck, dorsal skin, and axilla. In contrast, mice treated with control MC had a normal appearing thin epidermis and stratum corneum (Figure 5b). The skin observations were in keeping with a greater than 5,000 fold increase in keratin 16 (K16) mRNA, a marker of keratinocyte hyper-proliferation (Figure 5c). Dorsal skin excised from IL-17A MC injected mice revealed the formation of a mixed inflammatory infiltrate consisting of polymorphonuclear leukocytes (Munro's microabscesses) in the upper dermis associated around dilated capillaries with noted uniform epidermal hyperplasia (Figure 5d). The mixed inflammatory infiltrates were absent in the GFP MC controls. These cutaneous observations in the IL-17A gene transfer cohort were correlated with a dramatic (up to 80% of all nucleated blood cells) increase in neutrophils within 24 hours of IL-17A gene transfer as detected by haematological analysis (Figure 5e). Transmission electron microscopy of dorsal skin also revealed the major ultrastructural features of IL-17A-induced epidermal hyperplasia, including hypertrophy and hyperplasia of the spinous layer with spongiosis and retained nuclei and compacted keratin filaments in the keratin layer. A mild uniform intercellular edema of the epidermis (Figure 5f), with retained nuclei in the upper epidermis (Figure 5g) and compact hyperkeratosis of the stratum corneum (Figure 5h) were prominent epidermal changes associated with elevated IL-17A that were absent in control mice.

DISCUSSION

The relevance of IL-23 and IL-17 in PsA is suggested by the elevation of IL-23, IL-17/IL-17R in psoriatic skin and synovial fluid from PsA patients [8, 25]. Single nucleotide polymorphisms in IL23A, IL23R as well as TRAF3IP2 (Act1), a downstream target of the IL-17 receptor (IL-17R), confer susceptibility to PsA, implying a central role of the IL-23/IL-17A axis in PsA pathogenesis [26, 27]. Since IL-23 regulates the differentiation of IL-17 producing T_H17 cells, it is hard to evaluate the significance of IL-17A in disease pathogenesis independently of IL-23 and other T_H17 related cytokines [28]. To address the direct role of IL-17A in psoriatic arthritis pathogenesis we employed a gene transfer approach to overexpress IL-17A in vivo, thereby dissecting IL-17A from the IL-23/T_H17 biology. IL-17A, consistent with previous reports, induced myelopoiesis and neutrophilia [29]. Serum analysis after 1, 3, 7 days and 7 weeks showed that only IL-17A was detectable within the first 72 hrs; however, other cytokines were also increased with chronic exposure to IL-17A. Notably, TNF was not significantly elevated even 7 weeks post-IL-17A gene transfer. Granulocyte macrophage activating factor (GM-CSF), a cytokine known to play a role in maintaining myelopoiesis in autoimmune diseases, was elevated 7 weeks post-gene transfer and although may play a role in perpetuating the myeloid signature it was not associated with the initial myelopoiesis [30, 31]. As there was no other cytokine apart from IL-17A directly associated with the expanded myeloid populations, our data clearly show a direct association between IL-17A and myelopoiesis in our model and confirm previous observations.

Interestingly, gene transfer of IL-17A induced serum TRAP and bone destruction as observed by micro-CT, in the absence of synovial inflammation. This was not associated with an increase in sRANKL but was associated with an expansion of an

IL-17R⁺CD11b⁺Gr1^{low}RANK⁺CSF-1R⁺ myeloid population. This expanded population in the IL-17A gene transfer mice included osteoclast precursors, which showed increased differentiation capacity to osteoclasts in vivo upon RANKL gene transfer relative to GFP controls. Similarly, in vitro cultures of CD11b⁺ cells sorted from IL-17A MC also showed a higher osteoclast differentiation capacity due to increased RANK and CSF1-R expression. Collectively our data clearly show that IL-17A-induced IL-17R⁺CD11b⁺Gr1^{low}RANK⁺CSF-1R⁺ osteoclast precursors exacerbate bone destruction in the absence of overt inflammation.

IL-17A^{-/-} mice are protected from joint disease in the CIA mouse model due to reduced anti-collagen antibody titer and collagen-specific T-cell proliferation, however, the role of IL-17A in initiating inflammatory arthritis remains elusive [32]. To test this, we performed the CIA model in female C57BL/6 mice, which are resistant in this particular experimental model of arthritis in mice overexpressing IL-17A or GFP[33]. IL-17A exacerbated the disease progression compared to GFP controls, and showed a strong upregulation of RANKL, TRAP and MMP9 mRNA, correlating with the osteoclast-related gene activation signature. Based on our findings, we propose that IL-17A has at least a dual effect in inflammatory arthritis. Firstly, IL-17A upregulates RANK on pre-osteoclasts making them hypersensitive to RANKL signal and secondly, IL-17A increases serum RANKL in the circulation. Collectively this set of data suggests a role of IL-17A in bone destruction in inflammatory arthritis.

Bone and joint destruction in IL-17A gene transfer coincided with skin pathology. Specifically, a diffuse epidermal hyperplasia (acanthosis) with associated compact hyperkeratotic and parakeratosis of the stratum corneum and formation Munro's microabscesses in the upper dermis were consistent with a greater than 5,000 fold increase in keratin 16 (K16) mRNA, a marker of keratinocyte hyper-proliferation. The skin pathology was absent in the GFP MC controls. These cutaneous observations in the IL-17A gene transfer cohort were correlated with a dramatic (up to 80% of all nucleated blood cells) increase in CD11b⁺Gr1^{high} neutrophils within 24 hours of IL-17A gene transfer as detected by haematological analysis and flow cytometry. A dense accumulation of CD11b⁺Gr1^{high} neutrophils commonly occurs in Munro's microabscess and their depletion reduces epidermal thickening and microabscess formation in flaky skin mice [34–36]. It is possible that IL-17A in addition to inducing the expansion of IL-17R⁺CD11b⁺Gr1^{low}RANK⁺CSF-1R⁺ subset also induces the expansion of a second myeloid cell subset, associated with the development of skin inflammation. Taken together, our data indicate that IL-17A can play a key role early on during the initiation stage of diseases involving bone and skin pathology such as psoriatic arthritis currently under investigation in proof-of-concept clinical trials [37].

Supplementary Material

Refer to Web version on PubMed Central for supplementary material.

Acknowledgments

The authors would like to thank Drake Laface and Hong Qiu for technical assistance with hydrodynamic delivery injections.

Funding

Research was partly supported by NIH research grant R01 AR062173 and SHC 250862 to IEA. ES is the recipient of NIH T32 CTSC predoctoral fellowship.

Glossary

IL-17A	Interleukin-17A
MC	minicircle
GFP	green fluorescent protein
PsA	psoriatic arthritis
RANKL	receptor activator of NF- κ B ligand
OPG	osteoprotegerin
M-CSF	macrophage-colony stimulating factor
TRAP	tartrate-resistant acid phosphatase

References

1. Anandarajah AP, Ritchlin CT. The diagnosis and treatment of early psoriatic arthritis. *Nat Rev Rheum.* 2009; 5(11):634–641.
2. Teitelbaum SL. Bone Resorption by Osteoclasts. *Science.* 2000; 289(5484):1504–1508. [PubMed: 10968780]
3. Lacey DL, Timms E, Tan HL, et al. Osteoprotegerin ligand is a cytokine that regulates osteoclast differentiation and activation. *Cell.* 1998; 93(2):165–176. [PubMed: 9568710]
4. Boyle WJ, Simonet WS, Lacey DL. Osteoclast differentiation and activation. *Nature.* 2003; 423(6937):337–342. [PubMed: 12748652]
5. Kotake S, Udagawa N, Takahashi N, et al. IL-17 in synovial fluids from patients with rheumatoid arthritis is a potent stimulator of osteoclastogenesis. *J Clin Invest.* 1999; 103(9):1345–1352. [PubMed: 10225978]
6. Harper EG, Guo C, Rizzo H, et al. Th17 cytokines stimulate CCL20 expression in keratinocytes in vitro and in vivo: implications for psoriasis pathogenesis. *J Invest Dermatol.* 2009; 129(9):2175–2183. [PubMed: 19295614]
7. Teunissen MB, Koomen CW, de Waal Malefyt R. Interleukin-17 and interferon-gamma synergize in the enhancement of proinflammatory cytokine production by human keratinocytes. *J Invest Dermatol.* 1998; 111(4):645–649. [PubMed: 9764847]
8. Chan JR, Blumenschein W, Murphy E, et al. IL-23 stimulates epidermal hyperplasia via TNF and IL-20R2-dependent mechanisms with implications for psoriasis pathogenesis. *J Exp Med.* 2006; 203(12):2577–2587. [PubMed: 17074928]
9. Adamopoulos IE, Tessmer M, Chao CC, et al. IL-23 is critical for induction of arthritis, osteoclast formation, and maintenance of bone mass. *J Immunol.* 2011; 187(2):951–959. [PubMed: 21670317]
10. Sherlock JP, Joyce-Shaikh B, Turner SP, et al. IL-23 induces spondyloarthritis by acting on ROR-gammat+ CD3+CD4-CD8- enthesal resident T cells. *Nat Med.* 2012; 18(7):1069–1076. [PubMed: 22772566]
11. Di Cesare A, Di Meglio P, Nestle FO. The IL-23/Th17 axis in the immunopathogenesis of psoriasis. *J Invest Dermatol.* 2009; 129(6):1339–1350. [PubMed: 19322214]

12. Nie H, Zheng Y, Li R, Guo TB, et al. Phosphorylation of FOXP3 controls regulatory T cell function and is inhibited by TNF-alpha in rheumatoid arthritis. *Nat Med.* 2013; 19(3):322–328. [PubMed: 23396208]
13. Lubberts E, Schwarzenberger P, Huang W, et al. Requirement of IL-17 Receptor Signaling in Radiation-Resistant Cells in the Joint for Full Progression of Destructive Synovitis. *J Immunol.* 2005; 175(5):3360–3368. [PubMed: 16116229]
14. van, Hamburg JP.; Corneth, OBJ.; Paulissen, SMJ., et al. IL-17/Th17 mediated synovial inflammation is IL-22 independent. *Ann Rheum Dis.* 2013; 72(10):1700–1707. [PubMed: 23328939]
15. Wang C, Wu L, Bulek K, et al. The psoriasis-associated D10N variant of the adaptor Act1 with impaired regulation by the molecular chaperone hsp90. *Nat Immunol.* 2013; 14(1):72–81. [PubMed: 23202271]
16. Sato K, Suematsu A, Okamoto K, et al. Th17 functions as an osteoclastogenic helper T cell subset that links T cell activation and bone destruction. *J Exp Med.* 2006; 203(12):2673–2682. [PubMed: 17088434]
17. Chen L, Wei XQ, Evans B, et al. IL-23 promotes osteoclast formation by up-regulation of receptor activator of NF-kappaB (RANK) expression in myeloid precursor cells. *Eur J Immunol.* 2008; 38(10):2845–2854. [PubMed: 18958885]
18. Adamopoulos IE, Chao CC, Geissler R, et al. Interleukin-17A upregulates receptor activator of NF-kappaB on osteoclast precursors. *Arthritis Res Ther.* 2010; 12(1):R29. [PubMed: 20167120]
19. El Malki K, Karbach SH, Huppert J, et al. An alternative pathway of imiquimod-induced psoriasis-like skin inflammation in the absence of interleukin-17 receptor a signaling. *J Invest Dermatol.* 2013; 133(2):441–451. [PubMed: 22951726]
20. Papp KA, Reid C, Foley P, et al. Anti-IL-17 receptor antibody AMG 827 leads to rapid clinical response in subjects with moderate to severe psoriasis: results from a phase I, randomized, placebo-controlled trial. *J Invest Dermatol.* 2012; 132(10):2466–2469. [PubMed: 22622425]
21. Gray EE, Ramirez-Valle F, Xu Y, et al. Deficiency in IL-17-committed V4 gammadelta T cells in a spontaneous Sox13-mutant CD45.1 congenic mouse substrain provides protection from dermatitis. *Nat Immunol.* 2013; 14(6):584–92. [PubMed: 23624556]
22. Kay MA, He CY, Chen ZY. A robust system for production of minicircle DNA vectors. *Nat Biotech.* 2010; 28(12):1287–1289.
23. Chao CC, Chen SJ, Adamopoulos IE, Davis N, Hong K, Vu A, et al. Anti-IL-17A therapy protects against bone erosion in experimental models of rheumatoid arthritis. *Autoimmunity.* 2011; 44(3):243–252. [PubMed: 20925596]
24. Teitelbaum SL, Ross FP. Genetic regulation of osteoclast development and function. *Nat Rev Gen.* 2003; 4(8):638–649.
25. Wilson NJ, Boniface K, Chan JR, et al. Development, cytokine profile and function of human interleukin 17-producing helper T cells. *Nat Immunol.* 2007; 8(9):950–957. [PubMed: 17676044]
26. Filer C, Ho P, Smith RL, et al. Investigation of association of the IL12B and IL23R genes with psoriatic arthritis. *Arthritis Rheum.* 2008; 58(12):3705–3709. [PubMed: 19035472]
27. Huffmeier U, Uebe S, Ekici AB, et al. Common variants at TRAF3IP2 are associated with susceptibility to psoriatic arthritis and psoriasis. *Nat Genet.* 2010; 42(11):996–999. [PubMed: 20953186]
28. Langrish CL, Chen Y, Blumenschein WM, et al. IL-23 drives a pathogenic T cell population that induces autoimmune inflammation. *J Exp Med.* 2005; 201(2):233–240. [PubMed: 15657292]
29. Schwarzenberger P, Huang W, Ye P, et al. Requirement of Endogenous Stem Cell Factor and Granulocyte-Colony-Stimulating Factor for IL-17-Mediated Granulopoiesis. *J Immunol.* 2000; 164(9):4783–4789. [PubMed: 10779785]
30. Codarri L, Gyulveszi G, Tosevski V, et al. RORgammat drives production of the cytokine GM-CSF in helper T cells, which is essential for the effector phase of autoimmune neuroinflammation. *Nat Immunol.* 2011; 12(6):560–567. [PubMed: 21516112]
31. El-Behi M, Ciric B, Dai H, et al. The encephalitogenicity of T(H)17 cells is dependent on IL-1- and IL-23-induced production of the cytokine GM-CSF. *Nat Immunol.* 2011; 12(6):568–575. [PubMed: 21516111]

32. Nakae S, Nambu A, Sudo K, et al. Suppression of immune induction of collagen-induced arthritis in IL-17-deficient mice. *J Immunol*. 2003; 171(11):6173–6177. [PubMed: 14634133]
33. Van de Velde NC, Mottram PL, et al. Transgenic mice expressing human FcγRIIIa have enhanced sensitivity to induced autoimmune arthritis as well as elevated Th17 cells. *Immunology letters*. 2010; 130(1–2):82–88. [PubMed: 20005897]
34. Steffen C. William John Munro and Munro's abscess, and Franz Kogoj and Kogoj's spongiform pustule. *The American Journal of dermatopathology*. 2002; 24(4):364–368. [PubMed: 12142621]
35. van der Fits L, Mourits S, Voerman JS, et al. Imiquimod-induced psoriasis-like skin inflammation in mice is mediated via the IL-23/IL-17 axis. *J Immunol*. 2009; 182(9):5836–5845. [PubMed: 19380832]
36. Schon M, Denzer D, Kubitz RC, et al. Critical role of neutrophils for the generation of psoriasiform skin lesions in flaky skin mice. *J Invest Dermatol*. 2000; 114(5):976–983. [PubMed: 10771480]
37. McInnes IB, Sieper J, Braun J, et al. Efficacy and safety of secukinumab, a fully human anti-interleukin-17A monoclonal antibody, in patients with moderate-to-severe psoriatic arthritis: a 24-week, randomised, double-blind, placebo-controlled, phase II proof-of-concept trial. *Ann Rheum Dis*. Published Online First: 29 January 2013. 10.1136/annrheumdis-2012-202646

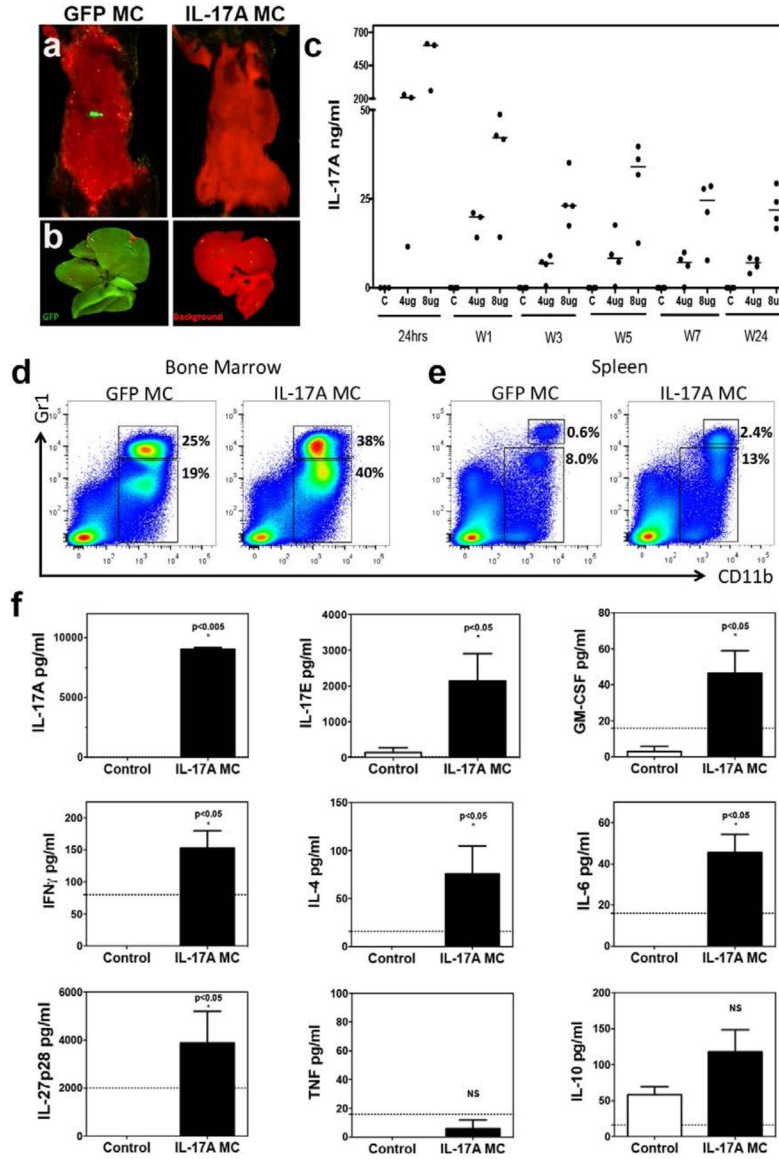


Figure 1. IL-17A gene transfer induces myelopoiesis

a) In vivo whole body and **b)** ex vivo 2D fluorescence imaging of C57BL/6 mouse liver explants one day post-gene transfer of IL-17A or GFP. Red denotes background and green GFP. **c)** Serum IL-17A levels, analyzed over 24 weeks showing stable expression after GFP or IL-17A MC transfer ($p < 0.0001$, Mann-Whitney non-parametric test; data pooled from three experiments). Flow cytometric analysis of **d)** bone marrow cells and **e)** splenocytes derived from GFP MC or IL-17A MC at day 3 depicting CD11b⁺Gr1⁺ cells (representative data of 3 experiments) **f)** Serum cytokine levels 7 weeks post IL-17A MC injection compared to GFP MC control mice. Data pooled from two independent experiments and 14 mice. (Dotted line shows sensitivity of each assay. $p < 0.05$ Mann-Whitney non-parametric test).

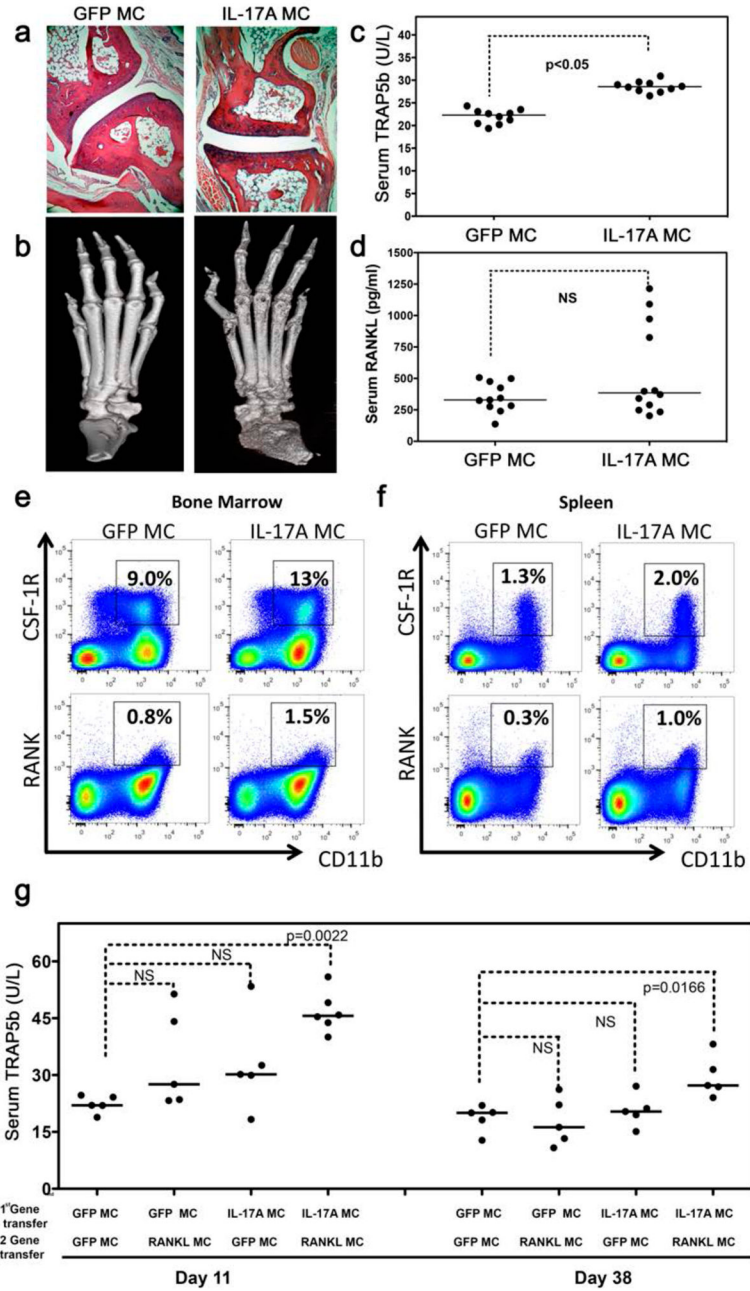


Figure 2. IL-17A induces an IL-17R⁺CD11b⁺Gr1^{low}RANK⁺CSF-1R⁺ osteoclast precursor and exacerbates RANKL-mediated osteoclastogenesis

a) H&E-stained decalcified limb samples from GFP MC and IL-17A MC-injected mice at 7 weeks post gene transfer showing no signs of synovial inflammation. Representative data from 4 experiments and 35 mice. **b)** Micro-CT 3D rendered images of paw anterior views post GFP-MC or IL-17A MC injection. Data representative of 4 experiments and a total of 10 analyzed mice. Serum **c)** TRAP5b and **d)** RANKL 3 weeks post gene transfer (each dot represents individual mice, data pooled from 3 experiments, $p < 0.05$ and NS respectively using students unpaired t-test). Flow cytometric analysis of **e)** bone marrow cells and **f)**

splenocytes derived from GFP or IL-17A gene transfer at day 3 depicting RANK⁺ and CSF-1R⁺ cells. Data is representative data of 3 experiments using 3 mice per experiment. **g)** Serum TRAP5b of mice 11 and 38 days post RANKL MC (0.05 µg) and GFP MC transfer in C57BL/6 mice overexpressing IL-17A or GFP for 30 days (each dot represent individual mice, data pooled from 2 experiments, students unpaired t-test).

Author Manuscript

Author Manuscript

Author Manuscript

Author Manuscript

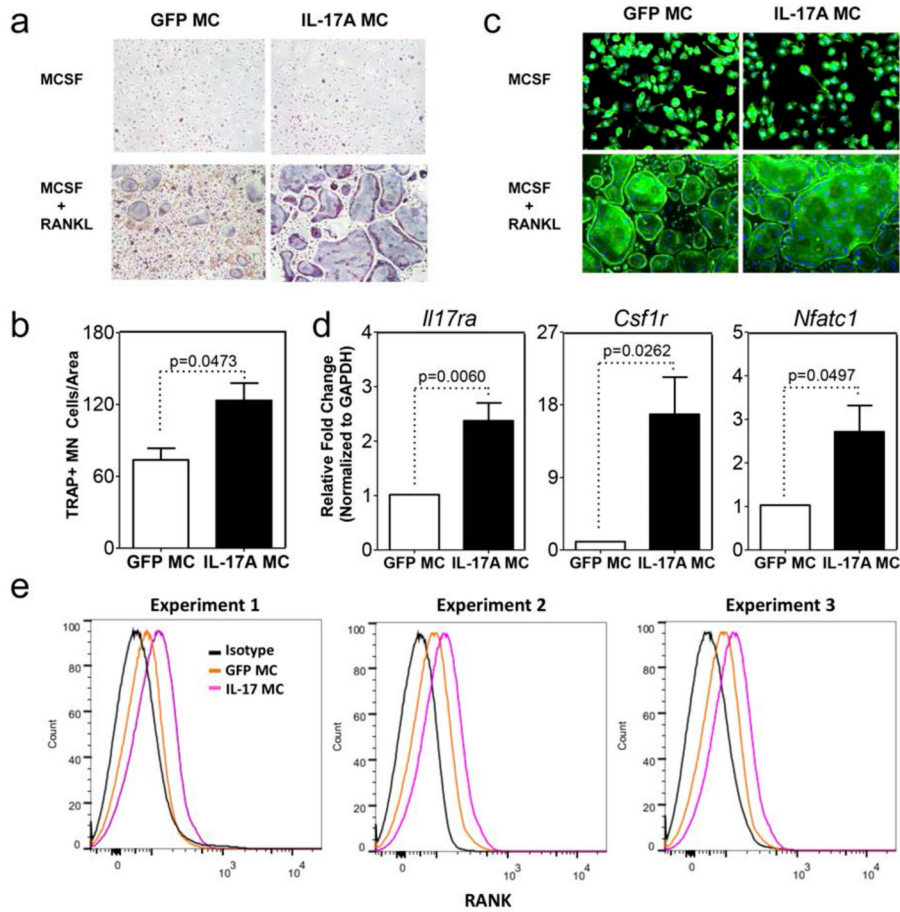


Figure 3. IL-17A induces osteoclast differentiation in a RANKL dependent manner *in vitro* TRAP **a**) cytochemical stain and **b**) quantitative analysis of TRAP⁺ multinucleated (MN) cells CD11b⁺ sorted bone marrow macrophages cells from GFP or IL-17A MC injected mice cultured for 4 days with M-CSF and RANKL. **c**) F-actin ring formation assay. Data for panel a and b are pooled from 4 experiments using 3 mice per group. **d**) qPCR of sorted RANK⁺ cells for expression of *Il17ra*, *csf1r* and *Nfatc1* normalized to *Gapdh* (data are pooled from 2 experiments using 3 mice per group). **e**) Flow cytometric analysis of RANK expression on cells extracted from bone marrow after GFP or IL-17A MC injection. Histograms are from 3 independent experiments. Black denotes isotype control, orange denotes GFP MC, and pink denotes IL-17A MC.

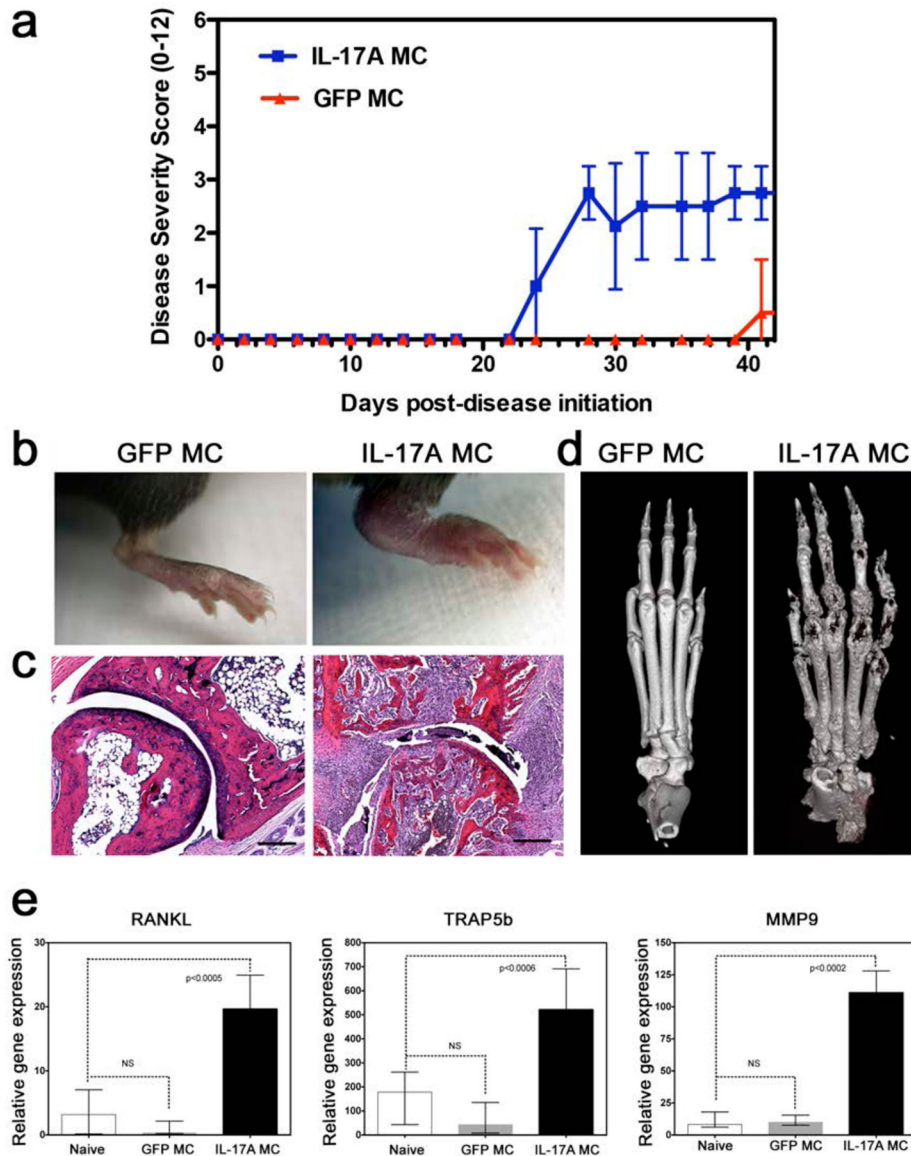


Figure 4. IL-17A exacerbates synovial inflammation and bone loss in inflammatory arthritis
a) Disease severity score of C57BL/6 mice post-gene transfer of IL-17A or GFP, immunized and challenged with bovine collagen type II. Data pooled from 2 experiments and a total of 20 mice analyzed. **b)** Representative photographic images of inflamed mouse paws post-GFP (left) and post-IL-17A (right) gene transfer at day 37 post collagen-induced arthritis initiation showing severe inflammation in the IL-17A gene transfer. **c)** H&E staining of tissue sections of paws showing infiltration of mononuclear cells, synovial lining cell hyperplasia, destruction of joint cartilage layers, and fibrous ankylosis post IL-17A gene transfer. **d)** Micro-CT of mouse paws showing severe bone erosion present in IL-17A MC (right) compared to GFP controls (left). **e)** Relative gene expression of RANKL, TRAP5b and MMP9 from mouse paws at 37 days post collagen-induced arthritis initiation (Data pooled from 4 mice).

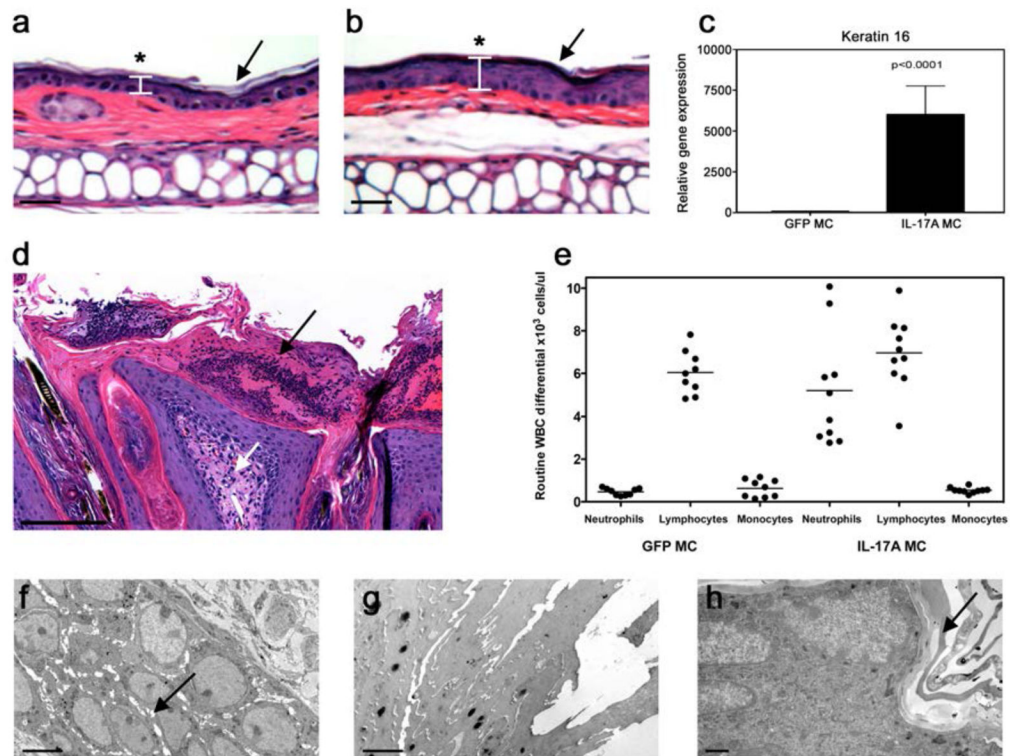


Figure 5. IL-17A induces skin pathology

H&E staining of cutaneous biopsies obtained from the ear 7 weeks post gene transfer of **a)** GFP MC or **b)** IL-17A demonstrating (asterisk) diffuse epidermal hyperplasia (acanthosis) with associated compact hyperkeratotic and parakeratosis of the stratum corneum (arrow) in IL-17A-treated mice (depicted by arrows, scale bar is 100µm). **c)** Relative gene expression of K16 from C57BL/6 dorsal skin 7 weeks post gene transfer demonstrating a greater than 5,000 fold increase in keratin 16 (data pooled from three experiments-students t-test). **d)** H&E staining of cutaneous biopsies obtained from dorsal skin 7 weeks post IL-17A gene transfer showing the presence of a mixed inflammatory infiltrate in the upper dermis associated around dilated capillaries (white arrow) and uniform epidermal hyperplasia. Prominent polymorphonuclear leukocytes in the epidermis; Munro's microabscesses (black arrow) (scale bar is 200µm). **e)** Flow cytometry (ADVIA) whole blood cell count of C57BL/6 mice 7 weeks post-gene transfer of both GFP and IL-17A showing a significant increase in neutrophil numbers in the IL-17A (right). Each dot represents individual mice, data collected from 3 individual experiments ($p < 0.0001$ one-way ANOVA). Transmission electron microscopy images of dorsal skin 7 weeks post IL-17A gene transfer showing the presence of **f)** mild uniform intercellular edema (arrow) of the epidermis with **g)** retained nuclei in the upper epidermis and compact hyperkeratosis of the stratum corneum. **h)** Control GFP-MC injected mice have a normal appearing epidermis with no intercellular edema and a thin stratum corneum (arrow). Scale bars for panels f, g, and h are 5µm.